Journal of Porous Materials 10: 31–39, 2003

Preparation and Characterization of Porous SiO_2-Al_2O_3-ZrO_2 Prepared by the Sol-Gel Process

R. MENDOZA-SERNA*
Facultad de Estudios Superiores Zaragoza, Carrera de Ing. Química, Universidad Nacional Autónoma de México, México, D.F. 09230, México
serna_mx@yahoo.com.mx

J. MÉNDEZ-VIVAR
Universidad Autónoma Metropolitana-Iztapalapa, Depto. de Química, A.P. 55-534, México, D.F. 09340, México

E. LOYO-ARNAUD
Facultad de Estudios Superiores Zaragoza, Carrera de Ing. Química, Universidad Nacional Autónoma de México, México, D.F. 09230, México

J.A. MORENO-RODRÍGUEZ
Universidad Autónoma Metropolitana-Iztapalapa, Depto. de Química, A.P. 55-534, México, D.F. 09340, México

P. BOSCH
Instituto de Investigación de Materiales, Universidad Nacional Autónoma de México, A.P. 70360, México, D.F. México

V.H. LARA
Universidad Autónoma Metropolitana-Iztapalapa, Depto. de Química, A.P. 55-534, México, D.F. 09340, México

Received August 29, 2002; Revised December 17, 2002

Abstract. An experimental strategy was developed to obtain Si—Al—Zr transparent sols via the sol-gel process. The sol was prepared from $Al(OBu^s)_3$ (OBu^s: $C_2H_5CH(CH_3)O$), $Zr(OPr^n)_4$ (OPr^n: $OCH_2CH_2CH_3$) and $Si(OEt)_4$. The chelating agents acetylacetone (2, 4 pentanedione, acacH), and itaconic anhydride (2-methylenesuccinic anhydride, anhH) were employed separately to stabilize Al and Zr precursors in order to control their chemical reactivity, avoiding precipitation. In all cases a prehydrolyzed tetraethyl orthosilicate (TEOS) sol was the Si source. We use the Partial Charge Model as a theoretical indication of the stabilization of the Al and Zr species derived from the reaction with anhH and acacH. The sols were polymerized at room temperature (293 K) to obtain gels and these were dried and calcined at 673, 773 and 873 K in air. The characterization techniques were Small Angle X-ray Scattering (SAXS), Fourier Transform Infrared Spectroscopy (FTIR), X-ray Diffraction (XRD), Thermal Gravimetric (TGA) and Differential Thermal Analyses (DTA). The porosity and surface area of solids calcined at 673, 773 and 873 K

*To whom correspondence should be addressed.

were determined by N_2 adsorption/desorption isotherms. The corresponding average pore diameter was evaluated using the methods BJH, HK and DA. These models were used because all together cover the full range of the pore size.

Keywords: chelating agents, SiO_2—Al_2O_3—ZrO_2, FTIR, XRD, porous materials

Introduction

The sol-gel route using metal alkoxides is of great interest in the preparation of homogeneous multicomponent glasses and thin films for technological applications [1, 2]. This method offers several advantages such as high purity of the final material, microstructure control, homogeneity at molecular scale, and low temperature preparation [3]. The starting components are usually alcoholic solutions of alkoxides which undergo condensation reactions after initial hydrolysis [4]. For preparation of SiO_2—Al_2O_3—ZrO_2 by the sol-gel method, TEOS, zirconium and aluminum alkoxides have been widely used as starting materials. However, the hydrolysis rate of zirconium and aluminum alkoxides are much faster than that of TEOS. The differences in structure and bond chemistry between those alkoxides (Si, Al, Zr) requires a careful procedure of hydrolysis and condensation of the mixed sols to tailor the structure at molecular scale. To circumvent this problem, many methods, including prehydrolysis of the silicon alkoxide, and modification of the zirconium and aluminum alkoxides separately, have been used [5]. The goal of this research was to obtain microporous SiO_2—Al_2O_3—ZrO_2 systems, based on a controlled hydrolysis-condensation process of the components. These materials are of interest in various areas of materials science such as alkali resistant glasses, chemically stable refractories, glass ceramics or zirconia toughened ceramics [6, 7]. The sols, gels, xerogels and oxides were obtained from a prehydrolized TEOS sol and Al and Zr alkoxides that were previously stabilized using anhH and acacH. The chelating agents were employed separately to stabilize the Al and Zr precursors. AcacH has often been reported in the sol-gel literature as a stabilizing agent for $Al(OBu^s)_3$ [8–10], and $Zr(OPr^n)_4$ [9–12]. The polymeric route has been previously used for the preparation of SiO_2—ZrO_2 [13], SiO_2—TiO_2 [14, 15] and SiO_2—TiO_2—ZrO_2 [16, 17]. Our experimental strategy allows to obtain interpenetrating oligomeric chains that lead to the formation of microporous structures, compared to a random close packing of particles, that would be obtained in a particulate system.

Experimental

Preparation of an A2 sol [17–19]

Chelating Agents. Two chelating agents (c.a.) were used to stabilize Al and Zr: 1. itaconic anhydride (2-methylenesuccinic anhydride, anhH) and 2. acetylacetone (2, 4 pentanedione, acacH). In all cases the molar ratio (c.a.)/M (M: Al, Zr) was 2.0.

Preparation of the Si—Al—Zr sol

A solution composed of acacH in EtOH was added to a sol containing $Al(OBu^s)_3$ dissolved in EtOH. The mol ratio acacH:Al was 2:1. AcacH dissolved in EtOH were added to a sol previously prepared, composed of $Zr(OPr^n)_4$ in EtOH. The mol ratio acacH:Zr was 2:1. The sol A2 was added dropwise to the chelating Zr sol (addition time: three hours). The Si—Zr sol was added dropwise to the chelating Al sol (addition time: four hours), to obtain the Si—Al—Zr sol. All the reactions were performed at room temperature (298 K). The sols were transparent and stable during the whole polymerization process. The molar ratio Si:Al:Zr was 80:7:13. The sol composition was calculated to obtain 5.0 wt. % of the corresponding oxides after calcination at 873 K.

Characterization Techniques

The Small Angle X-ray Scattering (SAXS) measurements were done with an equipment composed of a Kratky camera coupled to a copper anode tube. Nickel filters were employed to provide a wavelength selection which comprised a narrow band around the Cu K_α line. Small Angle X-ray curves were recorded with a position proportional counter. Data were analyzed as suggested in refs. [20–22].

The FTIR spectra of the sols were obtained using a spectrophotometer Perkin Elmer 1600 in the 4000–200 cm^{-1} region using nujol as the solvent. The samples were deposited between KBr plates and then analyzed. The FTIR study of xerogels and oxides calcined was performed using a spectrophotometer in the

4000–400 cm^{-1} region. KBr pellets were prepared grounding the samples in an agate mortar and mixing with anhydrous KBr in a weight ratio 10:1 KBr:sample, respectively.

X-ray diffractograms were obtained using a zirconium filtered molybdenum X-rays. High values of the angular parameter ($s = 4\Pi \sin\theta/\lambda$, where θ is the Bragg angle and λ the wavelength) were thus obtained. The intensity values, read at intervals $\Delta 2\theta = 1/8^\circ$ from $2\theta = 4^\circ$ to $2\theta = 70^\circ$, were the input data for the Magini and Cabrini program [23].

Thermal gravimetric (TGA) and differential thermal analyses (DTA) of powders were performed in a NETZSCH STA 409 EP equipment, in air atmosphere at 10 K/min heating rate, from 303 to 1273 K.

The N_2 adsorption/desorption isotherms of the xerogels calcined at 673, 773 and 873 K, were measured at 77 K in a Quantachrome Autosorb-3 after outgassing at 423 K for 12 h.

Results and Discussion

In order to clarify the discussion, the structures of acacH and anhH are presented in Fig. 1. The Partial Charge Model [24, 25] is based on the principle of electronegativity equalization stated by Sanderson [26, 27]. In this work we use the Partial Charge Model as a theoretical indication of the stabilization of the Al and Zr species derived from chelating with anhH and acacH, see Table 1. According to this principle, the criterion for stability of a ligand (i.e. anhH, acacH) bonded to a metal ion (i.e. Al, Zr) is given by its partial charge value (δ); the more negative this value, the more stable is the ligand bonded to the metal ion. The opposite occurs for ligands positively charged. In the present case we are using the partial charge model only as a first approach to try to explain the stability of the species formed once the chelating molecules bond to the alkoxides. As shown in Table 1, in all cases δ(anh) and δ(acac) values are negative indicating that anh^- and $acac^-$ are strongly bonded to Al and Zr, whereas the $\delta(OPr^n)$ values in Zr and $\delta(OBu^s)$ values in Al chelated with anhH and acacH are positive (results not shown here), and

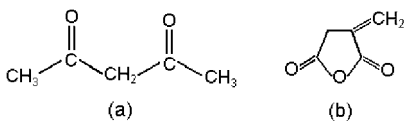

Figure 1. Chelating agents: (a) acetylacetone (acacH), and (b) itaconic anhydride (anhH).

Table 1. Partial charge (δ) values of bidentate Zr(VIII) and Al(VI) species chelated with acacH and anhH separately (c.a.: chelating agent).

Specie	δ(Zr)	δ(acac)	δ(Zr)	δ(anh)
$Zr(OPr^n)_4$	+0.7021	–	+0.7021	–
$Zr(OPr^n)_4(c.a.)_2$	+0.7347	−0.5399	+0.7727	−1.1691
$Zr(OPr^n)_3(c.a.)_2(H_2O)$	+0.7415	−0.4717	+0.7856	−1.0716
$Zr(OPr^n)_2(c.a.)_3$	+0.7498	−0.3884	+0.8219	−0.7978
$Zr(OPr^n)(c.a.)_3(H_2O)$	+0.7598	−0.2885	+0.8467	−0.6108
Especie	δ(Al)	δ(acac)	δ(Al)	δ(anh)
$Al(OBu^s)_3$	+0.4828	–	+0.4828	–
$Al(OBu^s)_3(c.a.)(H_2O)$	+0.5086	−0.6397	+0.5283	−1.3686
$Al(OBu^s)_2(c.a.)_2$	+0.5199	−0.5159	+0.5659	−1.0566
$Al(OBu^s)(c.a.)_2(H_2O)$	+0.5332	−0.3697	+0.5947	−0.8179

consequently very unstable. Upon hydrolysis the positively charged (Pr^nO) and (Bu^sO) species are easier to remove than the negatively charged (anh and acac) groups.

The fractal dimension (D_F) value of the fresh sols Si—Al(anh)—Zr(anh) and Si—Al(acac)—Zr(acac) were obtained from the Log I (h) vs. Log (h) plot. These Small Angle X-ray Scattering (SAXS) results indicate that linear oligomeric species were produced. The corresponding values were 1.70 and 1.81 respectively. The theoretical value of linear swollen oligomeric chains is 1.66 [13]. The form of the particles in the gels was estimated from the Kratky plot (Fig. 2). According to Kataoka et al. [28], if the Kratky curve presents a broad peak, the scattering particles most probably present a globular conformation; whereas if the curve approximates a plateau, the particles most probably are fibriform objects. According to these plots, in both cases the obtained oligomers are fibriform. These results agree with those obtained from SAXS, where linear chains were detected.

The FTIR bands assignment for the Si—Al(c.a.)—Zr(c.a.) sols is given in Table 2. The chelating of Al and Zr was detected in the fresh sols in the region 1381–1274 cm^{-1} when anhH was the chelating agent. The bands appeared at 1380–1280 cm^{-1} in the case of acacH (see Fig. 3). As expected, these bands decrease with thermal treatment of the samples (Figs. 3(b)–(c)), and completely disappear at 873 K (Fig. 3(d)). The evidence of Si—O—Al bond has also been demonstrated previously by ^{17}O [29], ^{29}Si [30, 31] and ^{27}Al NMR [32], whereas the Si—O—Zr bond has been demonstrated by ^{17}O NMR [33, 34]. In this research the Si—O—Al and Si—O—Zr bands, were clearly detected

Table 2. FTIR bands assignment in fresh Si—Al(c.a.)—Zr(c.a.) sols.

	Wavenumber (cm^{-1})	
Assignment	Si—Al(anh)—Zr(anh)	Si—Al(acac)—Zr(acac)
O—H stretching [35]	3339	3354
C—H stretching [36]	2968	2972
	2926	2930
O—H bending in free H_2O [37]	1639	1645
	1579	1594
CH_3 bending [38]	1456	1460
C—O—M stretching, (M: Zr, Al) [39]	1381	1380
	1334	1330
	1274	1280
O—H stretching in Si—OH [40, 41]	1154	1150
Si—O—Al [42, 43]	1080	1082
Si—O stretching in Si—O—Si disiloxane [39]	1053	1050
Si—OH stretching [44]	968	970
Si—O rings [41]	882	880
Si—O—Zr [16, 42]	793	796
Si—O—Si [41]	450	460

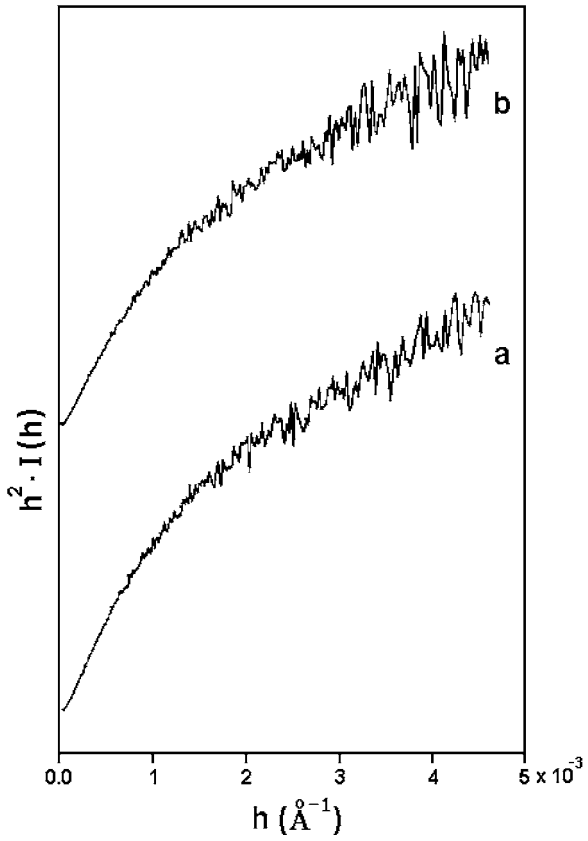

Figure 2. Kratky plot of the gels at room temperature (298 K): (a) Si—Al(anh)—Zr(anh) and (b) Si—Al(acac)—Zr(acac).

in all the FTIR spectra of the sols. These bands appeared in the fresh Si—Al(acac)—Zr(acac) sol at 1082 cm^{-1} and 796 cm^{-1}, respectively, and it gradually disappeared in the xerogel (Fig. 3(b)) and the solids calcined (Figs. 3(c)–(e)) due to the proximity of the Si—O—Si intense band at 1050 cm^{-1}.

The Si—Al(anh)—Zr(anh) and Si—Al(acac)—Zr(acac) powders analyzed by X-ray diffraction were found to be amorphous even after thermal treatment at 873 K. The XRD patterns of the Si—Al(anh)—Zr(anh) powders are shown in Fig. 4. Weak reflections on zirconia were identified only after calcining at 1173 K; see Fig. 4(d). Similar results were obtained for the Si—Al(acac)—Zr(acac) samples. These results indicate that the powders structure was stable up to 873 K. Regarding the DTA and TGA results of Si—Al(anh)—Zr(anh) (Fig. 5), the weight loss was slowly completed at 973 K. The first weight loss occurred at 303–473 K (8%). It was accompanied by a weak endothermal peak at 393 K. These changes are due to the elimination of solvent and H_2O [35]. The second weight loss occurred at 473–973 K (40%) and it was accompanied of an exothermal peak at 693 K that corresponds to the burning of organic residue [45]. Similar results were obtained for Si—Al(acac)—Zr(acac).

The isotherms for the Si—Al(acac)—Zr(acac) at 673, 773 and 873 K appear in Fig. 6. The samples exhibit an isotherm type I [46, 47] indicating that micropores are present along with mesopores. Type I isotherms are exhibited by microporous solids having relatively small external surface. Sintering occurred during this calcining temperature range (673–873 K) as the adsorbed volume gradually decreased; particularly between 773 and 873 K (see Fig. 6). This temperature range corresponds to the elimination of organic residue. The corresponding adsorption-desorption isotherms of Si—Al(anh)—Zr(anh) (results not shown here) show a low hysteresis in the desorption branches, that can be interpreted as the existence of smooth and cylindrical pores. The *t*-Plot of data confirmed the presence of micropores, because positive intercepts were obtained [48], the corresponding values for Si—Al(acac)—Zr(acac) were 3.5, 17.5 and

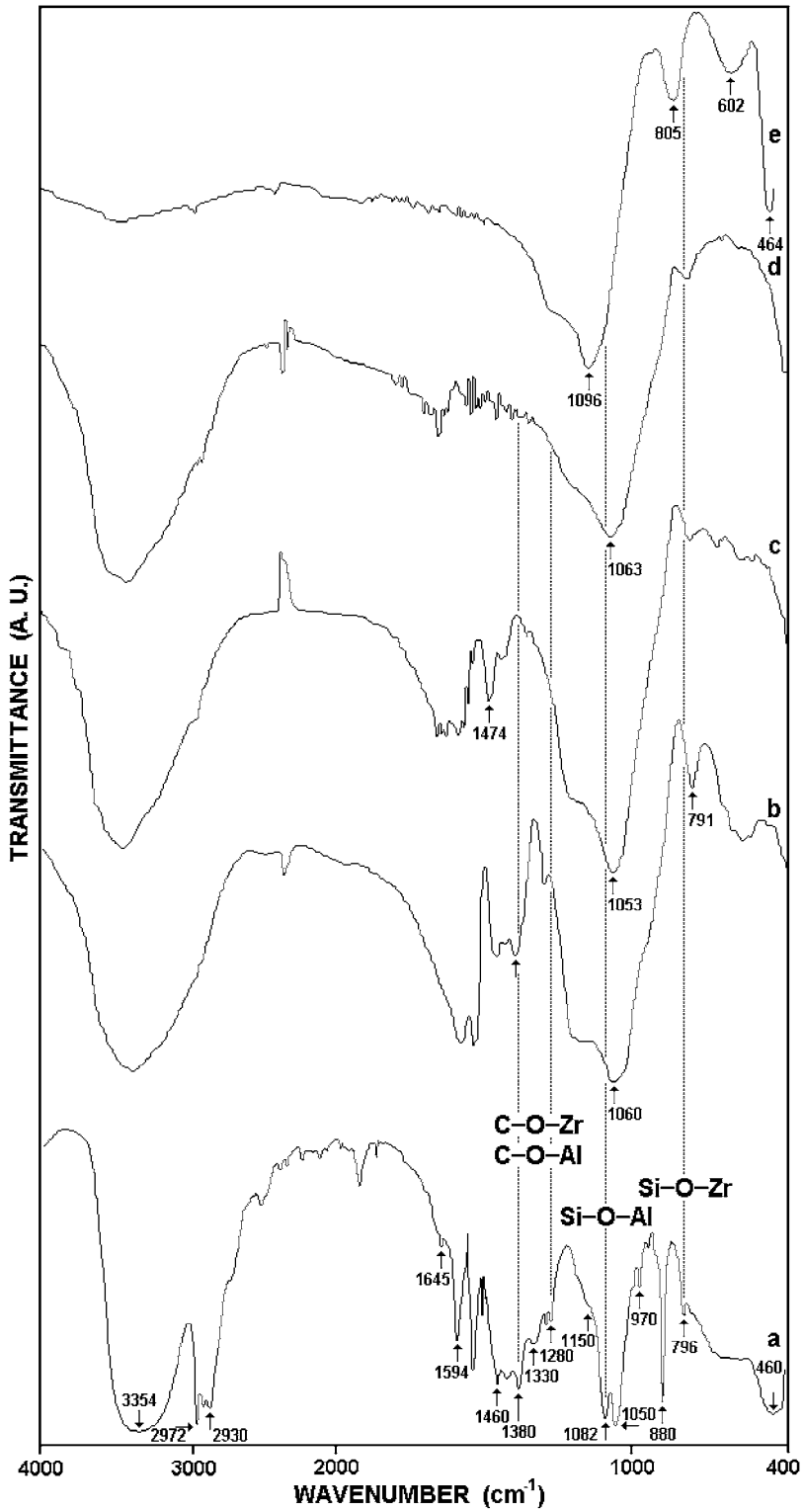

Figure 3. FTIR spectra of Si─Al(acac)─Zr(acac): (a) fresh sol, (b) xerogel dried at 423 K, and solids calcined at: (c) 573 K, (d) 873 K and (e) 1173 K.

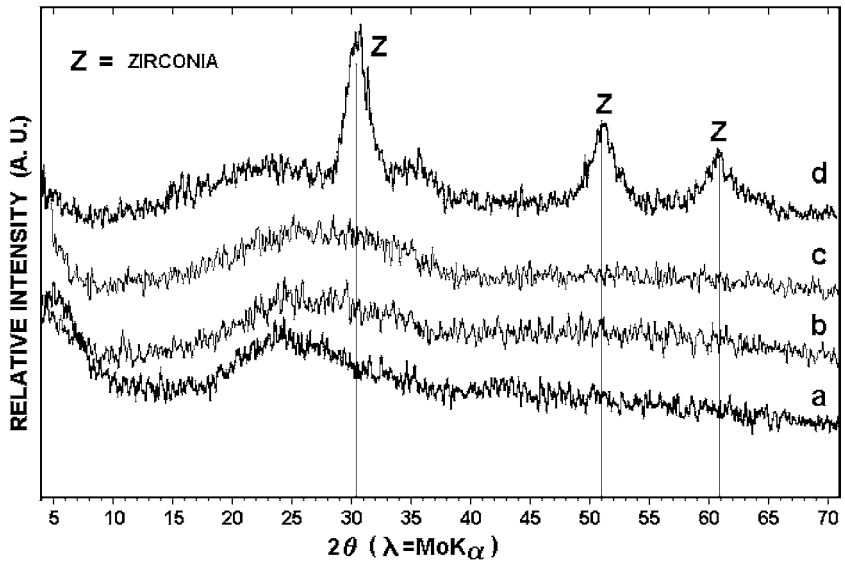

Figure 4. X-ray powder diffraction patterns of Si—Al(anh)—Zr(anh) at: (a) 423 K, (b) 573 K. (c) 873 K, and 1173 K.

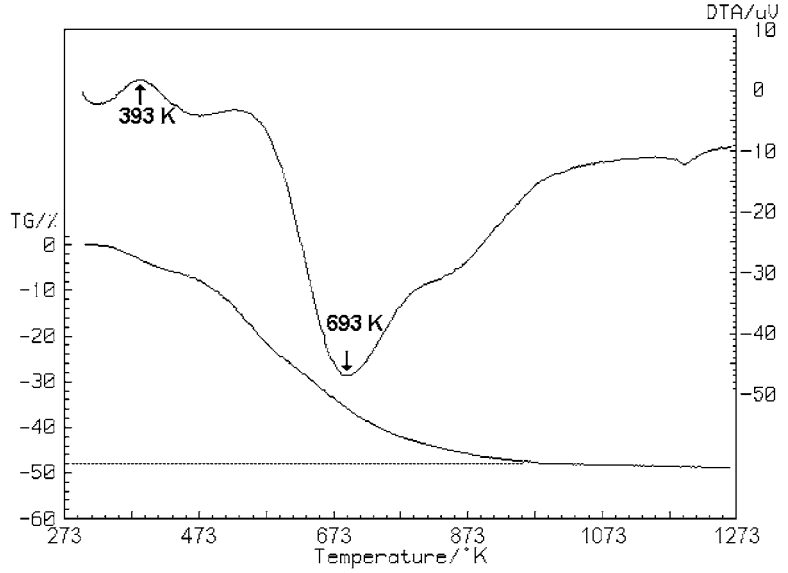

Figure 5. DTA/TGA curves of Si—Al(anh)—Zr(anh).

19.0 for the solids calcined at 673, 773 and 873 K, respectively. The pore size distribution in the micropore zone was evaluated using the methods proposed by Horváth-Kawazoe (HK) [49], and Dubinin-Astakhov (DA) (see Fig. 7). There is a widening of the pore size distribution with the thermal treatment; this result confirms the sintering observed in the isotherms. The pore size distribution in the mesopore zone was evaluated using the method proposed by Barret, Joiner and Halenda (BJH) [50]. The results appear in Table 3. The BET surface area of the xerogels calcined at 673, 773 and 873 K of the Si—Al(acac)—Zr(acac) samples were 63, 59 and 14 m^2/g respectively, while the Langmuir surface area were 100, 95 and 23 m^2/g respectively. Regarding the HK and DA methods, the average pore diameter of the samples was found to be smaller than 2.0 nm. The surface area reduction and the further size growth of the pores with the thermal treatment are caused by

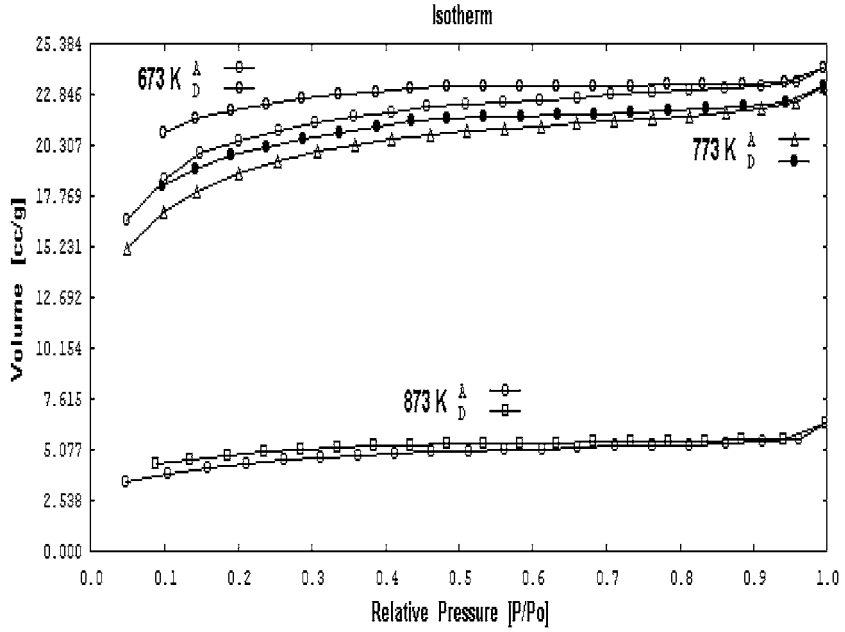

Figure 6. Nitrogen adsorption/desorption isotherms for Si—Al(acac)—Zr(acac) at 673, 773 and 873 K.

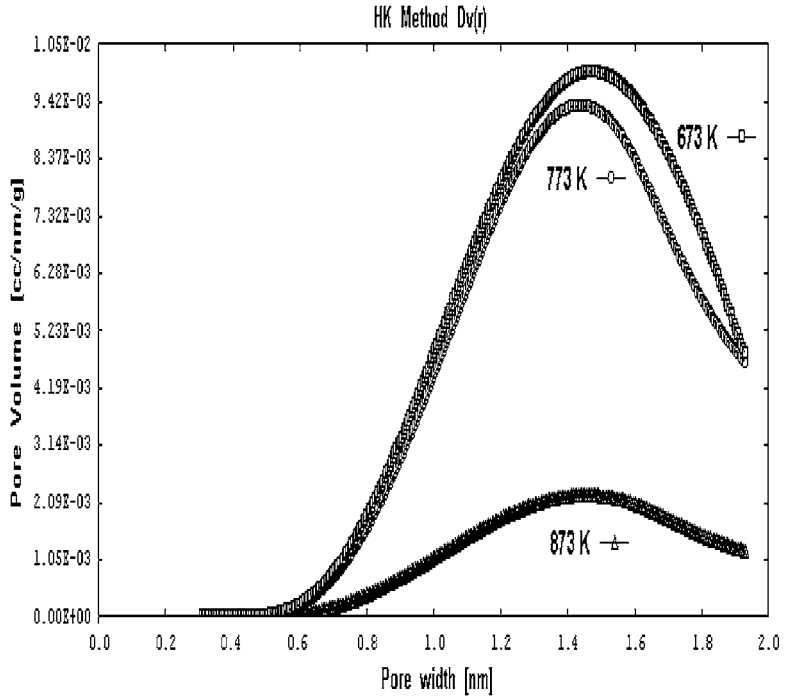

Figure 7. Pore size distribution of Si—Al(acac)—Zr(acac) at 673, 773 and 873 K according to the Horváth-Kawazoe model.

the elimination of organic residue. Larger surface area values were obtained when acacH was the modifying agent (see Table 3), indicating that it bonds strongly to Al and Zr and retards sintering. This was not the case for anhH, as a low surface area was initially obtained and a dramatic reduction occurred at 773 K. In addition, the average pore diameter of Si—Al(acac)—Zr(acac) were smaller compared to Si—Al(anh)—Zr(anh). According

Table 3. Porosimetry data of the Si─Al(c.a.)─Zr(c.a.) samples.

Sample	Temperature (K)	BET surface area (m^2/g)	Langmuir surface area (m^2/g)	Average pore diameter (nm) method		
				BJH	HK	DA
Si─Al(anh)─Zr(anh)	673	27	43	1.6	1.5	1.6
	773	2	5	2.4	1.8	1.9
	873	–	–	2.7	1.8	1.8
Si─Al(acac)─Zr(acac)	673	63	100	1.7	1.5	1.7
	773	59	95	1.7	1.4	1.7
	873	14	23	1.6	1.5	1.8

to these results, acacH is a better stabilizing agent for Al and Zr, compared to anhH.

Conclusions

The use of monomeric Al and Zr precursors and the prehydrolysis of TEOS ensured the homogeneity of the sols, gels, xerogels and oxides obtained up to 873 K. The experimental strategy allowed to obtain linear oligomeric species, according to the SAXS results and the Kratky plots. The formation of the Si─O─Al and Si─O─Zr bands and their stability was demonstrated by FTIR spectroscopy. Although sintering was observed in the 673–873 K range, microporous solids were obtained when acacH was the modifying agent. Based on the surface area results and the average pore diameter values, acacH is a better stabilizing agent of Al and Zr in these systems, compared to anhH. The partial charge model calculations can be used only as a preliminary indication of the species stability.

Acknowledgments

R.M.-S. and E.L.-A. gratefully acknowledge U.N.A.M., DGAPA (Grant PAPIIT No. IN104901) for the financial support. We thank L. Castillo-Granada for the FTIR analyses.

References

1. C.J. Brian, M.C. Tessie, R.W. Cruse, and R.M. Mininni, in *Better Ceramics Through Chemistry IV*, **180**, Materials Research Society Symposium Proceedings, 727–732 (1990).
2. D. Gyongjuan and G.H. Frischat, J. Sol-Gel Sci. Tech. **13**, 763 (1998).
3. C.J. Brinker and G.W. Scherer, *Sol-gel Science, The Physics and Chemistry of sol-gel Processing* (Academic Press, San Diego, CA, 1990), 839–841.
4. Ch. Wies, K. Meise-Gresch, W. Müller-Warmuth, W. Beier, A.A. Göktas, and G.H. Frischat, Ber. Bunsenges. Phys. Chem. **92**, 689 (1988).
5. K.Ch. Song, J. Sol-Gel Sci. Tech. **13**, 1017 (1998).
6. M. Popa, J.M. Calderón-Moreno, L. Popescu, M. Kakihana, and R. Torecillas, J. Non-Cryst. Solids **297**, 290 (2002).
7. K.V. Damodaran, V.S. Nagarajan, and K.J. Rao, J. Non-Cryst. Solids **124**, 233 (1990).
8. J.C. Debsikdar, J. Mater. Sci. **20**, 4454 (1985).
9. D. Hoebbel, T. Reinert, H. Schmidt, and E. Arpac, J. Sol-Gel Sci. Tech. **10**, 115 (1997).
10. W.C. LaCourse and S. Kim, Ceram. Eng. Sci. Proc. **8**, 1128 (1987).
11. J.B. Miller, S.E. Rankin, and E.I. Ko, J. Catal. **148**, 673 (1994).
12. Z. Zhan and H.C. Zeng, J. Non-Cryst. Solids **243**, 26 (1999).
13. J. Méndez-Vivar and C.J. Brinker, J. Sol-Gel Sci. Tech. **2**, 393 (1994).
14. J. Méndez-Vivar, R. Mendoza-Serna, J. Gómez-Lara, and R. Gaviño, J. Sol-Gel Sci. Tech. **8**, 235 (1997).
15. J. Méndez-Vivar, R. Mendoza-Serna, P. Bosch, and V.H. Lara, J. Non-Cryst. Solids **248**, 147 (1999).
16. J. Méndez-Vivar, R. Mendoza-Serna, and L. Valdez-Castro, J. Non-Cryst. Solids **288**, 200 (2001).
17. L. Valdez-Castro, J. Méndez-Vivar, and R. Mendoza-Serna, J. Porous Mater. **8**, 303 (2001).
18. J. Méndez-Vivar and R. Mendoza-Serna, Scanning, **20**, 347 (1998).
19. R. Mendoza-Serna, P. Bosch, J. Padilla, V.H. Lara, and J. Méndez-Vivar, J. Non-Cryst. Solids **217**, 30 (1997).
20. O. Glatter, Acta Physica Austr. **47**, 83 (1977).
21. O. Glatter, J. Appl. Cryst. **10**, 415 (1977).
22. H.P. Klug and L.E. Alexander, *X-Ray Diffraction Procedures for Polycristalline and Amorphous Materials*, 2nd edition (John Wiley & Sons, NY, 1974), p. 837.
23. M. Magini and A. Cabrini, J. Appl. Cryst. **5**, 14 (1972).
24. J. Livage and M. Henry, in *Ultrastructure Processing of Advanced Ceramics*, edited by J.F. Mackenzie and D.R. Ulrich (Wiley, New York, 1988), p. 183.
25. C. Sanchez, J. Livage, M. Henry, and F. Babonneau, J. Non-Cryst. Solids **100**, 65 (1988).
26. R.T. Sanderson, Science **114**, 670 (1951).
27. R.T. Sanderson, Inorg. Chem. **25**(19), 3518 (1986).
28. M. Kataoka, J.M. Flanagan, F. Tokunaga, and D.M. Engelman, *Use of X-ray solution Scattering for Protein Folding Study in*

Synchrotrom Radiation in the Biosciences, edited by B. Chanse, J. Deisenhofer, S. Ebashi, D.T. Goodhead, and H.E. Huxley (Clarendon Press, Oxford, UK, 1994), Vol. 4, p. 87.
29. I. Jaymes, A. Douy, P. Florian, D. Massiot, and J.P. Coutures, J. Sol-Gel Sci. Tech. **2**, 367 (1994).
30. T.-C. Sheng, S. Lang, B.A. Morrow, and I.D. Gay, J. Catal. **148**, 341 (1994).
31. J.C. Pouxviel and J.P. Boilot, *Ultrastructure Processing of Advanced Ceramics*, edited by J.D. Mackenzie and D.R. Ulrich (John Wiley & Sons, USA, 1988), p. 197.
32. J.C. Pouxviel, J.P. Boilot, A. Dauger, and L. Huber, in *Better Ceramics Through Chemistry II*, edited by C.J. Brinker, D.E. Clark, and D.R. Ulrich (Mat. Res. Soc. Symp. Proc. **73**, 1986), p. 269.
33. F. Babonneau, in *Better Ceramics Through Chemistry VI*, edited by A.K. Cheethan, C.J. Brinker, M.L. Mecartney, and C. Sanchez (Mat. Res. Soc. Symp. Proc. **346**, 1994), p. 949.
34. P.J. Dirken, R. Dupree, and M.E. Smith, J. Mater. Chem. **5**(8), 1261 (1995).
35. A. Duran, C. Serna, V. Fornes, and J.M. Fernández Navarro, J. Non-Cryst. Solids **82**, 69 (1986).
36. K. Nakamoto, *Infrared and Raman Spectra of Inorganic and Coordination Compound*, 5th ed. (John Wiley & Sons, USA, 1997), p. 356.
37. J. Méndez-Vivar, A. Campero, J. Livage, and C. Sánchez, J. Non-Cryst. Solids **121**, 26 (1990).
38. M. Sedlar and M. Sayer, J. Sol-Gel Sci. Tech. **10**, 115 (1997).
39. C.J. Pouchert (Ed.), *The Aldrich Library of Infrared Spectra*, 3rd ed. (Aldrich Chemical, Milwaukee, WI, 1981), p. 252.
40. T. López, J. Méndez-Vivar, T. Zamudio, and M. Villa, Mater. Chem. Phys. **30**, 161 (1992).
41. C.J. Pouchert (Ed.), *The Aldrich Library of Infrared Spectra*, 3rd ed. (Aldrich Chemical, Milwaukee, WI, 1981), p. 246.
42. Y. Abe, N. Sugimoto, Y. Nagao, and T. Misono, J. Non-Cryst. Solids **108**, 150 (1989).
43. T.-C. Sheng, S. Lang, B.A. Morrow, and I.D. Gay, J. Catal. **148**, 341 (1994).
44. C.J. Brinker and G.W. Scherer, *Sol-gel Science; The Physics and Chemistry of sol-gel Processing* (Academic Press, San Diego, CA, 1990), p. 544.
45. P.F. James, J. Non-Cryst. Solids **100**, 93 (1988).
46. S. Lowell and J.E. Shields, *Powder Surface Area and Porosity*, 3rd Edition (Ed. B. Scarlett, Chapman & Hall, 1991), p. 72.
47. S.J. Gregg, K.S.W. Sing, *Adsorption, Surface Area and Porosity* (Academic Press London 1982), chap. 4, 195–247.
48. R.S. Mikhail, S. Brunauer, and J. de Boer, J. Colloid Interface Sci. **26**, 45 (1968).
49. G. Horvát and K. Kawazoe, J. Chem. Eng. Japan, **16**(6), 470 (1983).
50. E.P. Barrett, L.G. Joyner, and P.P. Halenda, J. Am. Chem. Soc. **73**, 373 (1951).